Water Science
ScienceDirect
Water Science 29 (2015) 123–133
journal homepage: www.elsevier.com/locate/wsj

# LiDAR-based predictions of flow channels through riparian buffer zones

A.G. Solomons [a], E.A. Mikhailova [a,*], C.J. Post [a], J.L. Sharp [b]

[a] *Department of Forestry and Environmental Conservation, Clemson University, Clemson, SC 29634, USA*
[b] *Department of Mathematical Sciences, Clemson University, Clemson, SC 29634, USA*

Received 1 October 2015; received in revised form 25 November 2015; accepted 26 November 2015
Available online 15 January 2016

**Abstract**

Riparian buffer zones (RBZs) are critical for protecting stream water quality. High Resolution Light Detection and Ranging (LiDAR) data provides a way to locate channels where water can flow through a RBZ and into a stream. The objectives of this study were to characterize flow channels through riparian buffer zones around Lake Issaqueena, SC, USA, using LiDAR topography models and to validate these predictions using field observations of channel presence, soil moisture content and soil temperature. A LiDAR derived digital elevation model (DEM) was utilized to define flow channels and determine forty sample locations. Analysis indicated channel locations and the presence of large forested buffers generally 10 m or greater in the study area. High flow accumulation channels can be accurately predicted by LiDAR data, but lower flow channels were less accurately estimated. Surface soil temperature measurements were relatively uniform showing no difference between predicted channel and control locations. Presented methodologies can serve as a template for future efforts to quantify riparian buffers and their effects on protecting water quality.


*Keywords:* Geographic Information Systems (GIS); Riparian buffer zone (RBZ); Soil moisture; Thermal imagery; Water quality; Watershed management

## 1. Introduction

Most riparian buffer characterization efforts using remote sensing data have focused on using low-resolution data to understand areas adjacent to streams. Typically, 30 m resolution Landsat satellite data is used for the analysis along with digital elevation models (DEMs) with a similar resolution (Narumalani et al., 1997). Using this relatively low-resolution data is problematic because the size of the buffer is typically similar to the size of each individual pixel

* Corresponding author at: Department of Forestry and Environmental Conservation, Clemson University, 261 Lehotsky Hall, Clemson, SC 29634, USA. Tel.: +1 864 656 3535; fax: +1 864 656 3304.
*E-mail address:* eleanam@clemson.edu (E.A. Mikhailova).
Peer review under responsibility of National Water Research Center.

Production and hosting by Elsevier

http://dx.doi.org/10.1016/j.wsj.2015.11.001

(30 m) and therefore fails to represent buffer characteristics in smaller areas. Stream buffer analysis also does not typically account for areas where water flows through the buffer zone to the stream (James et al., 2007). LiDAR data, which comes from plane mounted instruments, measures three-dimensional surface characteristics by determining the canopy, understory, and surface topography using reflected light from rapidly emitted laser pulses (Wasser et al., 2015). In order to better understand the RBZ dynamics and what constitutes each buffer, higher resolution and more accurate data need to be used. James et al. (2007) observed that buffer zones may be so heavily forested that analysis by satellite imagery or conventional remote sensing techniques may not be efficacious. Use of LiDAR based data may be an effective way to identify channels that may be otherwise hidden from view (James et al., 2007).

Location and contribution of channels that flow through RBZs into streams is critical because they contribute to the overall health of the stream (Johansen et al., 2010a). Having a buffer around perennial or permanent streams is important but locating areas where water is flowing into the stream through RBZs is also a significant issue when considering stream health (Johansen et al., 2010a). Studies by Lee et al. (2000) and Sabater et al. (2003) demonstrated that RBZs are critical in preventing sediment, excess nutrients, and toxic metals from flowing into a stream. While the need to protect permanent or perennial streams is generally recognized and is the subject of numerous laws and regulations, the protection of ephemeral channels that are only present during or shortly after storm events is largely unregulated (Clean Water Act, 1972). These channels, which frequently can provide a direct path for sediments, nutrients, and other materials to flow into a stream during a storm event with little or no interaction with a riparian buffer. Locating these channels may improve understanding of RBZs functioning and identify more effective buffers to improve stream health and subsequent water quality.

Soil moisture levels may be a way to identify ephemeral channels (Creed et al., 2008). Visible water may not be present on the soil surface but water may be maintained in the soil structure, giving areas with ephemeral channels higher average soil moisture then non-channel locations. Modern instruments for soil moisture determination are an effective and accurate way to analyze the water content present in the soil (Vaz et al., 2013).

Field evaluation and analysis of buffer zone characteristics of ephemeral, or intermittent streams is possible based on visual analysis of ground topography but it is important to identify techniques that may allow for standardized channel detection. Ground-based thermal imagery collection has been used successfully in the field to identify areas of saturated soil and water connectivity and dynamics in the landscape (Pfister et al., 2010). In addition, laboratory studies of soil temperature have been successfully able to predict different types of soil permeability (de Lima et al., 2014). Detection of moist soil using thermal imaging is possible because evaporative cooling effects causes a temperature change which can be detected at the soil surface.

The objectives of this study are: (1) to characterize the riparian buffer zones system by identifying channel presence that traverse buffers; (2) to characterize buffer size using LiDAR data and compare this to field observations; (3) to validate potential differences in LiDAR predicted channel locations versus ground conditions via field observation, soil moisture content and soil temperature.

## 2. Materials and methods

### 2.1. Study area

Lake Issaqueena is located in the Savannah River Basin area of Pickens County in the upstate region of South Carolina (Fig. 1). The lake is classified as being in the Piedmont region which follows the area south of the Appalachian Mountains (United States Geological Survey, 2012). The project study area (approximately 12 km$^2$) is predominantly a mixed hardwood forest with areas of planted pines (*Pinus* spp.). The land was reclaimed in the 1930s from a degradated soil area caused by poor farming practices that caused an almost total loss of topsoil. The study area is almost completely within the boundaries of the Clemson University Experimental Forest with the exception of a small amount of privately owned land. Lake Issaqueena is fed by one fourth-order stream, Six-Mile Creek, two third-order streams, Indian Creek and Wildcat Creek as well as numerous ephemeral and intermittent streams. For the data collection, the majority of the sample points occur in the Clemson Forest, however, four of the points on the eastern branch of Lake Issaqueena were outside of the boundaries of the Clemson Experimental Forest. The topography of the area is varied with slopes ranging from 5% to 25%. Vegetation is dense, especially around the streams where dense groves of mountain laurel (*Kalmia latifolia* L.) form a canopy over most of the streams.

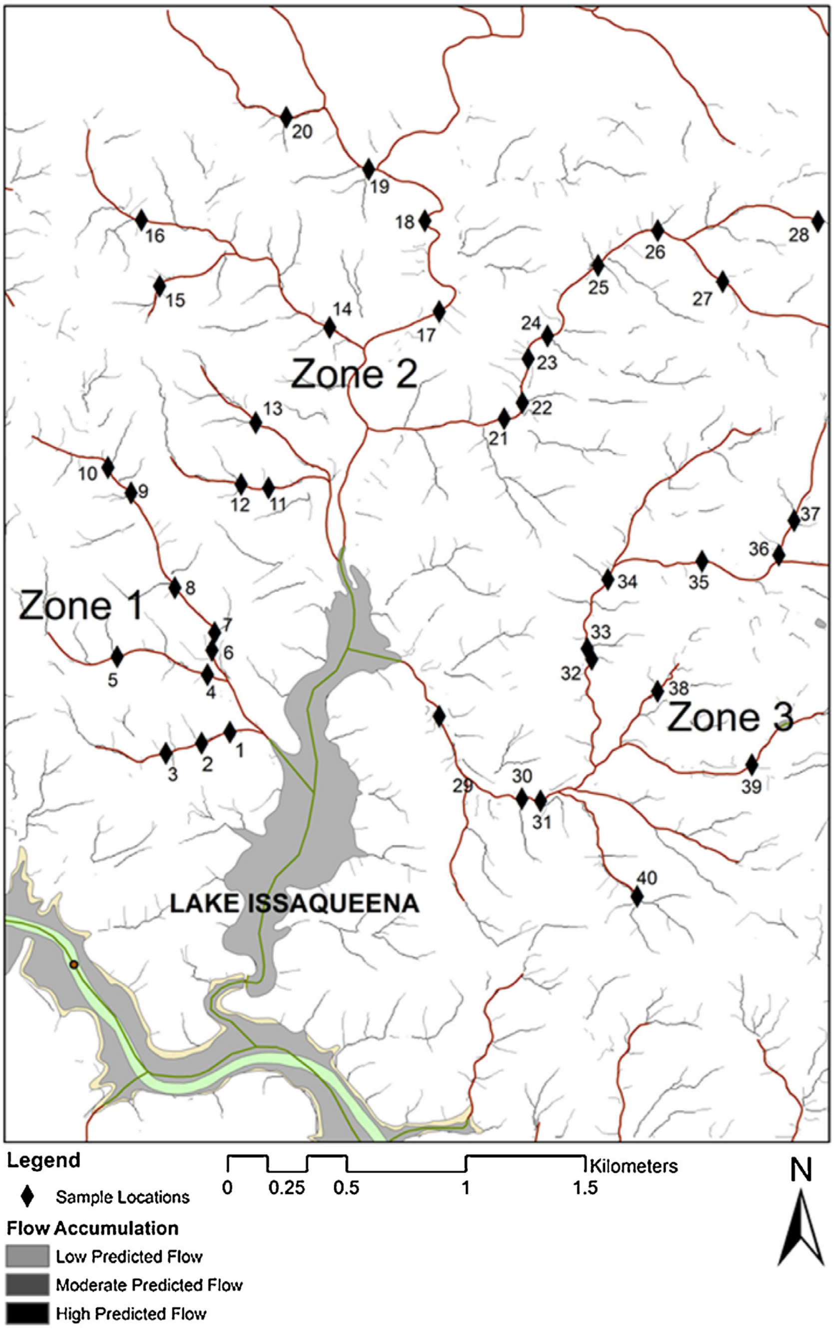


Fig. 1. Lake Issaqueena study area (latitude: 34°44′06″ N; longitude: 82°51′52″ W). Zones represent different stream networks.

### 2.2. LiDAR data and processing

Light Detection and Ranging (LiDAR) based data was used to define both the topography and stream buffer characteristics for this study (Fig. 2 and Table 1). The remote sensing LiDAR data (which was used for the buffer analysis and was the data source for the DEM) was clipped to the study area and has an approximate spacing of 1 return/m$^2$ and a vertical and horizontal accuracy of approximately 20 cm. A pre-existing LiDAR based DEM was used to represent ground topography (with a 3.048 m cell size and similar accuracy to the LiDAR), while standard

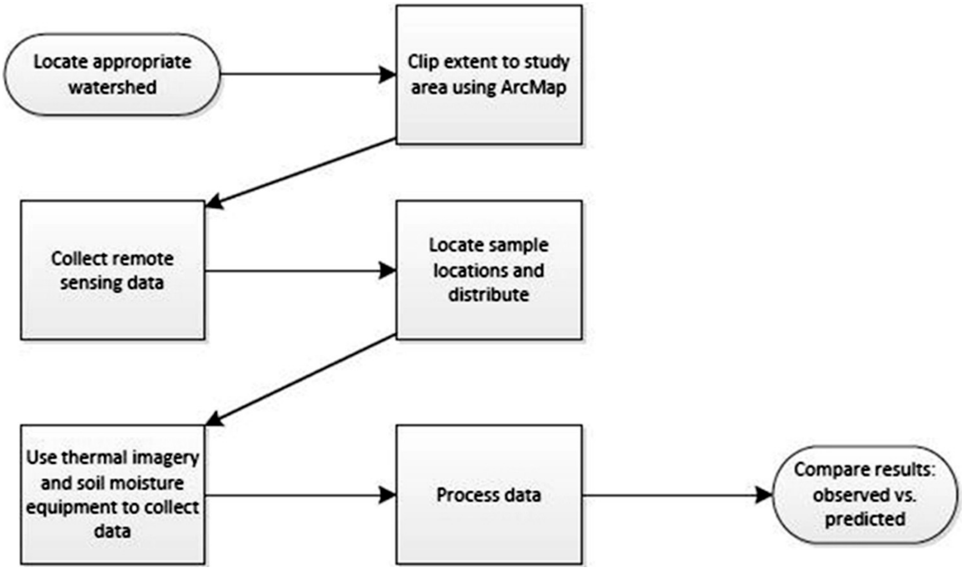


Fig. 2. Flowchart of processes.

Table 1
Data sources and descriptions.

| Data layer | Source | Coordinate system | Date |
|---|---|---|---|
| LiDAR (LAS) files | Pickens County GIS | NAD State Plane 1983 SC | 2011 |
| Lake Polygon | Pickens County GIS | NAD State Plane 1983 SC | 2013 |
| Hydrology Datasets | USGS NHD | NAD State Plane 1983 SC | 2012 |

flow accumulation routines within the Spatial Analyst extension of ArcGIS 10.2.2 (ESRI, 2011) were used to map ephemeral channels. The DEM cell size was chosen based on the posting of the origininal LiDAR data. The flow accumulation channels flowing into the perennial streams were identified and arranged into three different categories (1, 2, or 3) based on the unique accumulation value of each identified pixel ArcMap provided (low, medium, and high accumulation). A LiDAR derived Digital Terrain Model (DTM) using first-return data was used to estimate buffer presence to compare to the field measurements.

### 2.3. Sample location determination

Sampling locations (Fig. 1) were determined by finding points where the LiDAR-DEM indicated water flow intercepting an identified perennial stream from United States Geological Survey (USGS) National Hydrologic Dataset (NHD) (United States Geological Survey, 2012; Fig. 2 and Table 2). Each sample point had an assigned value correlating to the amount of flow accumulation that the LiDAR-DEM indicated. Of the 122 potential locations in the study area, 40 were randomly determined. The sample area was divided into three sampling zones: Zone 1, Zone 2, and Zone

Table 2
Characterization of sample locations along streams near Lake Issaqueena, SC.

| Parameters | Units | Zone 1 | Zone 2 | Zone 3 |
|---|---|---|---|---|
| Stream order | – | 4th | 3rd | 3rd |
| Channel category (flow level) | | | | |
| Category 1 (“Low”) | 0.46–0.93 ha contributing area | 4 | 4 | 2 |
| Category 2 (“Medium”) | 0.93 –1.39 ha contributing area | 2 | 4 | 4 |
| Category 3 (“High”) | Above 1.39 ha contributing area | 4 | 10 | 6 |

Fig. 3. Example of Category 3 (“high” flow level) channel.

3 (Fig. 1). A representative number of predicted channel sampling locations were selected from each zone: 10 from “low” (Category 1) flow level, 10 from “medium” (Category 2) flow level, and 20 from “high” (Category 3) flow level. The Category 1 (“low” flow) channel represented a contributing area of between 0.46 and 0.93 ha, while the Category 2 (“medium” flow) had a contributing area between 0.93 and 1.39 ha and the Category 3 (“high” flow) channels had a contributing area ranging from 1.39 and above. Stratified sampling generation within SAS® (version 9.3, SAS Institute Inc., 2011) was conducted on stream branch and category with probabilities similar to the proportion of sites in each section and category. Ten samples were selected from Zone 1, 18 samples were selected from Zone 2, and 12 samples were selected from Zone 3. Sampling locations were randomly drawn from the stratified sample (Fig. 3).

### 2.4. Field data collection

The data obtained from the sampling map, along with stream data layers (United States Geological Survey, 2012) were used to populate a geodatabase where it was the base map for GIS-based field data collection with ArcCollector (ESRI, Redlands, CA) with an android tablet (Google Nexus 7, second generation; Table 3). A custom data entry form with attributes was created for the purpose of easily recording data measurements in the field. The Global Positioning System (GPS)-capable tablet, using the ArcCollector software, recorded the current location for accurate sampling and data which could be easily entered into the collection form (Fig. 4).

### 2.5. Thermal image data collection

Thermal images provided one of the methods tested to determine the presence of ephemeral or intermittent channels. A low-cost thermal camera Seek XR™ (about $300) was used to image soil temperature. The camera interfaced to the

Table 3
Field and GIS measured parameters, Lake Issaqueena, SC.

| Parameter | Units | Instrument |
|---|---|---|
| Channel presence | Categorical data (1 = low flow; 2 = medium flow; 3 = high flow) | Visual |
| Soil moisture of channel | Volumetric water content (1–100) | FieldScout TDR 300 Soil Moisture Meter |
| Soil moisture of control | Volumetric water content (1–100) | FieldScout TDR 300 Soil Moisture Meter |
| GPS location | Latitude/longitude | Garmin 72H GPS |
| Thermal image of channel | Fahrenheit | Seek Thermal XR |
| Thermal image of control | Fahrenheit | Seek Thermal XR |
| Bearing of thermal image[a] | Categorical data (1–10) | Suunto compass |
| Buffer width | Meter (m) | Meter stick |
| Buffer composition of channel | Categorical data | Visual |
| Field data entry | N/A | Google Nexus tablet with ArcCollector for Android |

[a] *Note*: Used to identify sample location.

Google Nexus tablet through its micro-USB connector and an included application provided by the camera manufacturer was used to acquire and save thermal imagery. The thermal camera has a temperature range from −40 °C to 330 °C and an infrared range from 7.2 μ to 13 μ. (Seek Thermal™, 2015). A thermal picture was taken after surface debris was removed exposing bare soil. "Cooler" temperature colors, such as blue, indicated cooler temperatures on the soil surface. A "cool" temperature in comparison to a warmer control temperature may indicate that water is present in the soil (Pfister et al., 2010). In addition to the color, a temperature value was given (ranging from 66 °F to 95 °F or 18.3 °C to 35.0 °C) which was uploaded into ArcCollector. The data were compared to control points, which were pre-determined to be 10 m (based on field determination of typical distance between channels in this area) away from the actual sample location and away from LiDAR DEM-predicted flow channels. A control thermal picture was taken in the same way as at the sample locations.

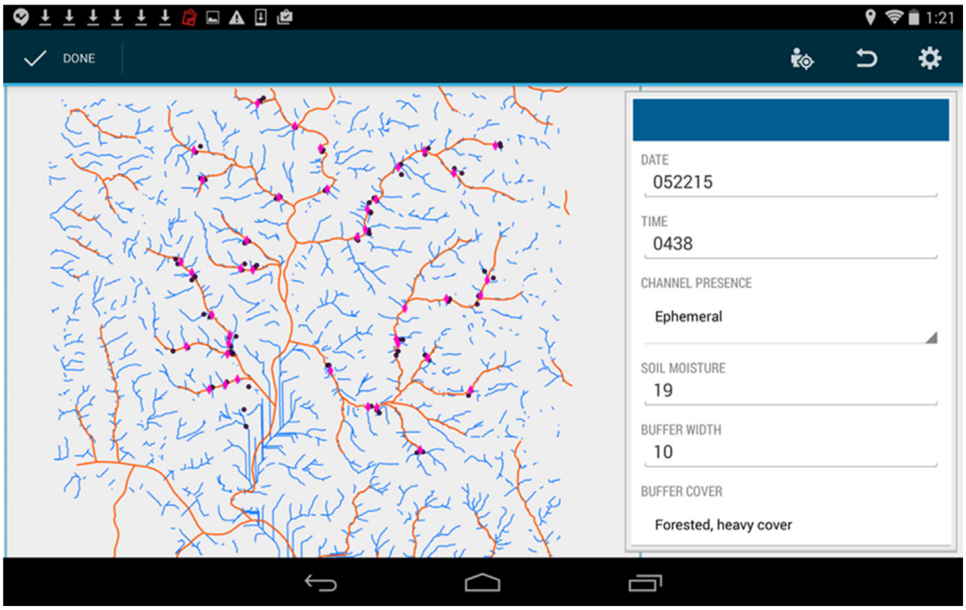


Fig. 4. Example of ArcCollector interface.

### 2.6. Riparian buffer zone characterization

The RBZs were characterized by estimating the density of vegetation around each of the stream channels both by field visits and LiDAR analysis: vegetated buffer with dense overstory; vegetated buffer with moderately dense overstory; vegetated buffer with little or no overstory, and predominately bare soil.

A significant amount of information was already known about the types of buffers surrounding the streams from analysis of LiDAR data, and previous visual analysis of site characteristics. The width of the immediate buffer zone was calculated in meters.

### 2.7. Determination of channel presence using soil moisture

Soil moisture was also used as a parameter to identify where soil moisture had accumulated in the soil. An electromagnetic soil moisture meter (FieldScout TDR 300®, Spectrum Technologies Inc., 2015) with 7.62 cm rods was used to determined soil water content as percent volumetric water content. At each sample location, a measurement was recorded and then a control sample was taken 10 m away in the same area as the control thermal image. The control data were collected in an area where LiDAR data indicated there was no flow accumulation. The soil moisture meter was calibrated after every 10 sample measurements. In addition, the moisture meter data was georeferenced through an interfaced handheld GPS (Garmin 72H®) which attached to the meter. Once the data measurements were taken, the data, including latitude and longitude, were recorded in a spreadsheet that was subsequently uploaded into Microsoft Excel. In addition, other variables were measured including: soil moisture of the channel, buffer width, buffer composition/type, and bearing.

### 2.8. Statistical methods

Soil moisture and temperature data were analyzed using SAS (SAS Institute Inc., 2011) to compare site versus control averages for each category using paired sample tests. Tests of significance were evaluated with a $\alpha = 0.05$ significance level.

## 3. Results

### 3.1. Characteristics of channels through riparian buffer zones

Table 4 shows the number of channels that were observed in the field by noting areas where channels bypassing the RBZs were visually obvious. Six channels out of a possible 10 were observed in Category 1 and 2 ("low" and "medium" flow level). Eighteen out of a possible 20 channels were observed in Category 3 ("high" flow level). At the time of sampling, no LiDAR indicated channels had any water present on the surface. The weather around the time of sampling had been dry for several days leading to the lack of surface water.

### 3.2. Characteristics of riparian buffer zones

Table 5 shows the relationship between stream flow levels, buffer width and buffer cover composition around Lake Issaqueena. The buffers were generally wide with a mean of 8.8 m and standard deviation of 2.4 m and had dense vegetation cover, except where sample locations lied on private property.

Table 4
Comparison of observed versus LiDAR predicted channels around Lake Issaqueena.

| Ephemeral channel (predicted channel category/flow level) | LiDAR predicted | Number in field verification |
|---|---|---|
| Category 1 ("Low") | 10 | 6 |
| Category 2 ("Medium") | 10 | 6 |
| Category 3 ("High") | 20 | 18 |
| Control | 0 | 0 |

Table 5
Stream category, buffer width, and buffer cover composition around Lake Issaqueena.

| Channel category (flow level) | Mean buffer width (stdev) (m) | Overall buffer composition | |
|---|---|---|---|
| | | Vegetative | Bare |
| Category 1 (“Low”) | 9.25 (2.05) | Dense | 0 |
| Category 2 (“Medium”) | 8.25 (2.76) | Dense | 0 |
| Category 3 (“High”) | 9.00 (2.38) | Dense | 0 |
| Overall | 8.83 (2.40) | Dense | 0 |

### 3.3. LiDAR data and validation

Table 7 summarizes the comparison between field validation (using soil moisture data) and the LiDAR predicted channel locations. LiDAR-based DEM data failed to accurately predict channels in low and medium flow accumulation channels ($\alpha = 0.05$, $p = 0.698$ and 0.5721, respectively). In high flow accumulation channels, LiDAR was able to accurately predict channels ($\alpha = 0.05$, $p = 0.0003$). Buffer measurements based on a LiDAR canopy height model (CHM) were similar overall to the field measurements (Table 6). The CHM was used to determine if tree cover was present or absent from a cell in order to measure buffer width. There were some difficulties identifying buffer width with the CHM because of the 3.043 m resolution of the raster cells.

### 3.4. Thermal imagery

Table 8 shows descriptive statistics for the thermal imagery data. The observed locations had a mean of 77.3 °F (25.2 °C) and the control locations had a mean of 79.9 °F (26.0 °C). The standard deviations for the observed locations were 4.9 °F (2.7 °C) and the control locations had a standard deviation of 5.2 °F (2.9 °C). The thermal imagery failed to identify channel presence as soil temperature was similar between observed sites and control sites with relatively large standard deviations. Fig. 5 demonstrates the variability of temperatures when a sample site is illuminated by direct sunlight versus a similar location where the ground is shaded by canopy cover. As Fig. 5 illustrates, sunlight has a powerful ability to heat soil when it is directly illuminated.

## 4. Discussion

Several studies have linked LiDAR data to channel presence (James et al., 2007; Johansen et al., 2010a,b). These studies are conclusive in the fact that LiDAR data has the ability to accurately locate the location of streams, however, this study agrees with the work of James et al. (2007) in that smaller channels may be more difficult for LiDAR data to predict. This study differs from previous studies in that it seeks to identify smaller channels that feed into larger streams using soil moisture content and thermal imagery as validation techniques. Use of a soil moisture meter is a novel technique in this field of study as its use is generally intended for agricultural or horticultural use. Thermal imagery is also a novel technique in that it has only recently come into more mainstream use because of price reduction and higher ease of use.

Table 6
Width of the riparian buffer zones around Lake Issaqueena: visual versus LiDAR predicted.

| Sampling zone | Visual | | LiDAR predicted | |
|---|---|---|---|---|
| | (*n*) | Mean width (stdev) (m) | (*n*) | Mean width (stdev) (m) |
| Zone 1 | 10 | 8.4 (2.9) | 10 | 8.0 (2.8) |
| Zone 2 | 12 | 7.8 (3.2) | 12 | 8.4 (3.3) |
| Zone 3 | 18 | 9.5 (1.5) | 18 | 8.9 (2.6) |
| Overall | 40 | 8.8 (2.5) | 40 | 8.4 (2.9) |

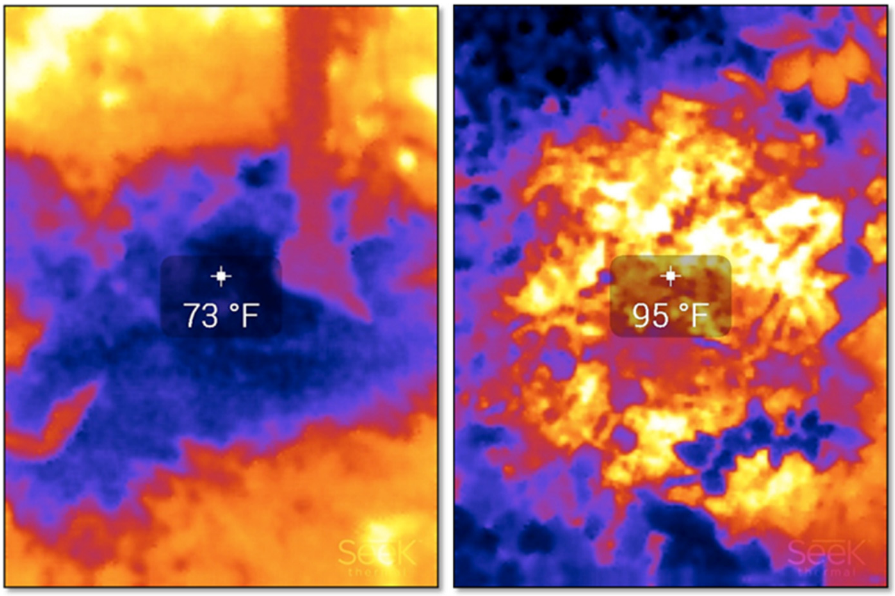


Fig. 5. Comparison between thermal image in sunlight (left) and similar location in shade (right).

Table 7
Summary statistics for soil moisture comparisons between LiDAR-predicted Category 1 ("low"), Category 2 ("medium"), and Category 3 ("high") stream flow (observed-predicted).

| Channel category (flow level) | *n* | DF | *t*-value | Pr > *t* | Mean (volumetric water content) | Standard deviation |
|---|---|---|---|---|---|---|
| Category 1 ("Low") | 10 | 9 | 2.06 | 0.0698 | 25.70 | 15.68 |
| Category 2 ("Medium") | 10 | 9 | 0.59 | 0.5721 | 16.20 | 6.17 |
| Category 3 ("High") | 20 | 19 | 4.41 | 0.0003 | 21.65 | 8.84 |
| Control | 40 | – | – | – | 15.03 | 4.26 |

Table 8
Summary statistics for thermal imagery data.

| Observed thermal mean (stdev) | Control thermal mean (stdev) |
|---|---|
| 77.3 °F (4.9 °F) | 79.9 °F (5.2 °F) |
| 25.2 °C (2.7 °C) | 26.0 °F (2.9 °C) |

### *4.1. LiDAR predictions of channels and buffer presence*

LiDAR offers an accurate method to map ground characteristics when compared to conventional methods of using aerial and satellite photography and visual analysis of ground topography. Field data shows that in this study only Category 3 ("high" flow) channels can be accurately predicted by use of LiDAR data when compared to visual identification (Table 4) and field measurements of soil moisture (Table 7). James et al. (2007) noted that larger features are accurately predicted by LiDAR data but that smaller features are not accurately predicted especially when features are small in size or run parallel to other features (James et al., 2007). Also, variations in the soil type (composition and texture) could produce small soil moisture sampling differences with the equipment readings (Vaz et al., 2013).

Buffer width estimations with a LiDAR canopy height model (CHM) were accurate overall, but there was likely some error because raster cells were identified as either have or not having tree cover and the 3.3 m cell size limited the resolution of the measurement.

### 4.2. Thermal data

The collected data suggest that thermal image data was not an accurate predictor of channel presence under study field conditions. It should be possible to use soil temperature to identify moist areas (Pfister et al., 2010) and controlled laboratory experiments have demonstrated a relationship between soil moisture and temperature (de Lima et al., 2014). Possible limitations of thermal imagery use in this study include the timing of the sample collection in relation to rain events (most sampling occurred during a dry period) and the differences in soil temperature caused by the variable presence of canopy cover shading direct sunlight.

## 5. Summary and conclusions

Flow accumulation analysis using the LiDAR-based DEM was excellent (90% accurate) at locating Category 3 ("high" flow) ephemeral or intermittent channels passing through the riparian buffer. For similar predicted channels with Category 1 and 2 ("low" or "medium" flow) the identification was less successful (60% accurate). This accuracy of channel prediction will likely vary depending on the density of the LiDAR used (and related DEM resolution and accuracy), so the accuracy of this type of analysis may improve with higher resolution LiDAR data. Control sites were accurately predicted as not having channels in all cases. Soil moisture data was able to distinguish the Category 3 ("high" flow) channels from surrounding areas, but similarly were unable to identify Category 1 ("low" flow) predicted channels. Analysis using a thermal camera was unsuccessful at finding channels with similar temperatures in the observed and control sites. There was also variation is soil temperature based on sun exposure of the sample site. Sampling times occurred in a generally dry period, and if it had been possible to sample directly after rain events, the thermal imagery may have been able to identify channels. Using a hand-held tablet with integrated GPS and data collection form worked well, but there was some uncertainty associated with the GPS accuracy, especially under heavy canopy. Future studies should consider incorporating a differentially corrected GPS.

## Acknowledgements

Data was provided by the USGS, USDA, and the Pickens County GIS office. Financial support was provided by Clemson University, Technical Contribution No. 6332 of the Clemson University Experiment Station. This material is based upon work supported by NIFA/USDA, under project numbers SC-1700452 and SC-1700462.

## References

Clean Water Act (CWA), 1972. EPA, Environmental Protection Agency, Available on-line at http://www.epa.gov/agriculture/lcwa.html.

Creed, I.F., Sass, G.Z., Wolniewicz, M.B., Devito, K.J., 2008. Incorporating hydrologic dynamics into buffer strip design on the sub-humid Boreal Plain of Alberta. For. Ecol. Manage. 256, 1984–1994.

de Lima, L.M.P., Abrantes, R.C.B., Valdemir Jr., P.S., Montenegro, A.A., 2014. Prediction of skin surface soil permeability by infrared thermography: a soil flume experiment. Quant. InfraRed Thermogr. J. 11, 161–169.

Environmental Systems Research Institute (ESRI), 2011. ArcGIS Desktop 10.2.2. Redlands, CA, pp. 2015.

James, L.A., Watson, D.G., Hansen, W.F., 2007. Using LiDAR to map gullies and headwater streams under forest canopy: South Carolina, USA. Catena 71, 132–144.

Johansen, K., Phinn, S., Wittle, C., 2010a. Mapping of riparian zone attributes using discrete return LiDAR, QuickBird and SPOT-5 Imagery: assessing accuracy and costs. Remote Sens. Environ. 114, 2679–2691.

Johansen, K., Arroyo, L.A., Armston, J., Phinn, S., Witte, C., 2010b. Mapping riparian condition indicators in a sub-tropical savanna environment from discrete return LiDAR data using object-based image analysis. Ecol. Indic. 10, 796–807.

Lee, K., Isenhart, T.M., Schultz, R.C., Mickelson, S.K., 2000. Multispecies riparian buffers trap sediment and nutrients during rainfall simulations. JEQ 29, 1200–1205.

Narumalani, S., Zhou, Y.C., Jensen, J.R., 1997. Application of remote sensing and geographic information systems to the delineation and analysis of riparian buffer zones. Aquat. Bot. 58, 393–409.

Pfister, L., McDonnell, J.J., Hissler, C., Hoffmann, L., 2010. Ground-based thermal imagery as a simple, practical tool for mapping saturated area connectivity and dynamics. Hydrol. Process. 24, 3123–3132.

SAS Institute Inc., 2011. Base SAS® Version 9.3. Cary, NC.

Sabater, S., Butturini, A., Clement, J.C., 2003. Nitrogen removal by riparian buffers along a European climatic gradient: patterns and factors of variation. Ecosystems 6, 20–30.

Seek Thermal Inc.™, 2015. Seek Thermal XR.

Spectrum Technologies Inc., 2015. FieldScout TDR 300 Soil Moisture Meter.
United States Geological Survey, 2012. National Hydrology Dataset.
Vaz, C., Jones, S., Meding, M., Tuller, M., 2013. Evaluation of standard calibration functions for eight electromagnetic soil moisture sensors. Vadose Zone J. 12, 1–16.
Wasser, L., Chasmer, L., Day, R.T., Allen, T., 2015. Quantifying land use effects on forested riparian buffer vegetation structure using LiDAR data. Ecosphere 6, 1–17.